JOURNAL OF MATERIALS SCIENCE 32 (1997) 1473–1477

A new method of fracture toughness determination in brittle ceramics by open-crack shape analysis

F. HAUBENSAK*, A. S. ARGON‡
Department of Mechanical Engineering, Massachusetts Institute of Technology, Cambridge, MA 02139, USA

Improvement of the fracture toughness of high-quality ceramics remains one of the most important goals in materials development. An associated problem is the accurate measurement of fracture toughness in such brittle or semi-brittle ceramics, particularly in small samples encountered in material development. Previously used methods relying on measurement of the size of fracture mirrors, the indentation load and crack length in Vickers hardness-induced cracking, and a variant of similar techniques, have all been less than satisfactory in discriminating quantitative differences among materials. A hitherto unused technique of inferring the fracture toughness in samples from measurements of open-crack flank displacements, which we have developed, avoids most of the theoretical and experimental difficulties of other methods. While it is somewhat intensive in terms of evaluation and requires high resolution of open cracks, the technique is fundamentally the soundest of all techniques and is capable of furnishing discriminating results. We present results of its application to the measurement of some model materials such as soda–lime glass, single-crystal silicon, alumina, and a reaction-bonded silicon nitride whose porosity would ordinarily present difficulties with other methods.

1. Introduction

In the development of materials with superior fracture toughness, the necessity of high resolution in the toughness measurements on small, laboratory-scale specimens is paramount. In this pursuit, a number of methods have been applied in the development of high-quality reaction-bonded porous silicon nitride (RBSN) produced by Haggerty *et al.* [1]. Nominally defect-free disc specimens initially were fractured in a ball-on-ring test configuration, and the fracture mirrors were measured and related to fracture toughness through the bend strength. These results showed broad trends, albeit with large uncertainty [2]. Standard indentation-toughness techniques, well described in the literature [3, 4], were also used, but proved to lack sensitivity. An experimental technique to pry open cracks emanating from circular holes in plate specimens produced excellent results in model materials, but was limited in use with the high stiffness silicon nitride material of interest. Large corrections in the induced displacements, due to compression of the wedging mechanism, while calculable, became larger than the actual displacements, with the result that inaccuracies became too large to be acceptable.

Finally, it is known that the crack-tip stress field can be deduced from the boundary conditions and the crack-flank opening displacements, if the elastic properties are known. Therefore, this methodology was developed further and for the special boundary value case of the internally pressurized half-penny shaped surface crack associated with the radial cracks of Vickers indentations. The development of this technique and its use in measuring K_{IC} in RBSN is the subject of the present communication.

2. Methodology

2.1. Theoretical preliminaries

In a Mode 1 crack-tip field for a crack under impending motion, $K_I = K_{IC}$ can be determined from

$$K_{IC} = \frac{(\mathrm{COD})\,E}{F(r/a)a^{1/2}} \tag{1}$$

where $F(r/a)$ is a non-dimensional characteristic crack-shape factor dependent on the geometry and the mode of loading, a is the crack length, and E is the Young's modulus. The function can be determined by finite element methods (FEM) for a crack of a given geometry and mode of loading under a unit K_1, $a^{1/2}$ and E. An example is presented in Fig. 1a for the case of a Vickers indentation of interest in an elastic, isotropic material. It was found that the shape of the open cracks qualitatively fit best with the solution of an internally loaded crack with point loads at the

* *Present address*: Intel Corp. D2 Technology Center, 2200 Mission College Blvd., Santa Clara, CA 95052-8119, USA.
‡ Author to whom all correspondence should be addressed.

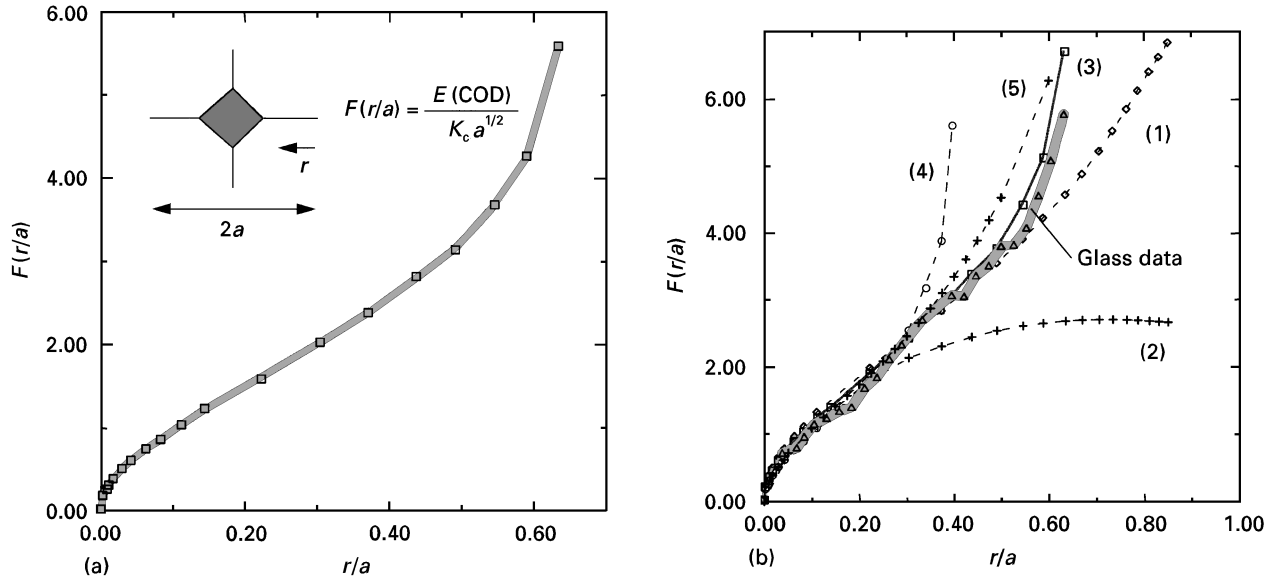

Figure 1 (a) The non-dimensional open-crack displacement function for an isotropic elastic two-dimensional material. In this calculation, the application of the point load dipole occurs at $r/a = 0.65$. (b) Comparison of various open-crack shape solutions for internally loaded surface cracks. Solution (1) is a centre loaded point force, (2) is for uniform internal pressure over the portion of the crack representing the indentation impression ($0.65a < r < a$), (3) is for symmetric point loading about the impression at $r/a = 0.65$, similarly (4) is for point loading at $r/a = 0.40$, and (5) is for a centrally loaded three-dimensional penny crack.

positions corresponding to the corners of the indentation. This can be seen in Fig. 1b, where various open-crack COD solutions are compared with measurements from indentations produced in a glass.

A fundamental assumption here is that indentation of material misfit or comminution chips under the indentor keep the crack open at the shape for its impending propagation. There are reasons to believe this to be the case in many circumstances [5–7], and various experimental observations [8], and analytical [9, 10] modelling support the notion that the residual stress state upon the removal of the indentation load is sufficient to extend the radial cracks during the unloading process to conditions of crack arrest.

Nevertheless, because of such possible relaxations from a critically stressed crack state, the determined fracture toughness values must be regarded as low toughness estimates.

2.2. Method of observation

Determination of the crack length and opening shape was done primarily by standard scanning electron microscopy (SEM) techniques, in order to attain high enough resolution, typically up to 2×10^4 magnification. However, other methods, such as atomic force microscopy and sometimes even light optical microscopy, have the potential to generate a similar quality of data.

Elastic properties were obtained either from the literature for the model materials, or were measured with a pulse-echo technique described elsewhere. [11].

2.3. Measurement of open-crack shapes from micrographs

While other methods exist for determining crack-flank opening displacements, a standard SEM was utilized for the measurements obtained here. The relative opening displacements were taken manually from the micrographs. Because the edges of the crack faces are not perfectly defined, upper and lower limits were estimated in the following manner. An upper limit was determined based on the notion that beyond a certain dimension, the contrast of the image does not change and represents the contrast of the surrounding solid. In the same way, the estimate of the lower limit was determined by considering the contrast inside the crack.

The resolution of the measurements is fundamentally limited by the resolution of the micrographs. However, the capability of measuring multiple crack-opening displacements permits this to be improved. Obtaining a well-documented shape of a single crack reduces the errors in comparison with a single measurement. Typical uncertainties associated with the measurement of the fracture toughness obtained from one crack, as defined by the standard error parameter, was found to be 3%.

2.4. Results of calibration experiments in standard materials

In order to determine the overall accuracy of the method, the measurement procedure was applied to three model materials: silica glass, an alumina single crystal and a silicon single crystal. The crack-opening displacement data are shown in Figs 2–4. The corresponding fracture toughness values are plotted in Fig. 5 for the data from the glass with the above described procedure, and shows an independence of the toughness with position along the crack. This implies a good match between the calculated and measured shape of the open-crack dimensions.

Furthermore, the numerical values of fracture toughness correspond well with the accepted values for the three model materials, as shown in Table I.

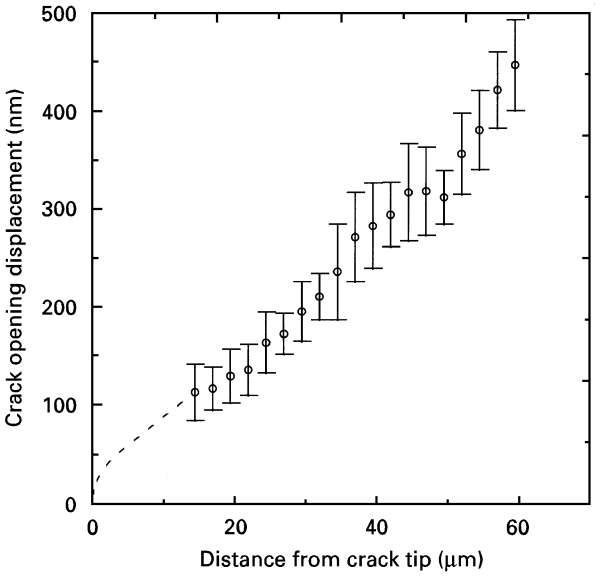

Figure 2 Open-crack displacement data from indentation induced cracks in silica glass.

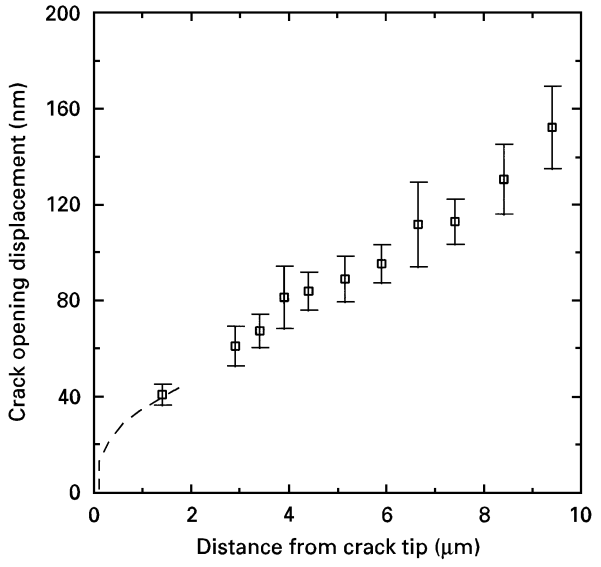

Figure 3 Open-crack displacement data from indentation induced cracks in single-crystal α-alumina.

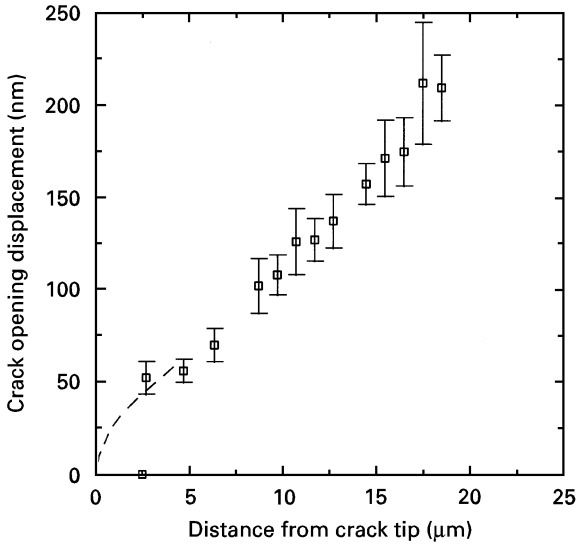

Figure 4 Open-crack displacement data from indentation induced cracks in single-crystal silicon.

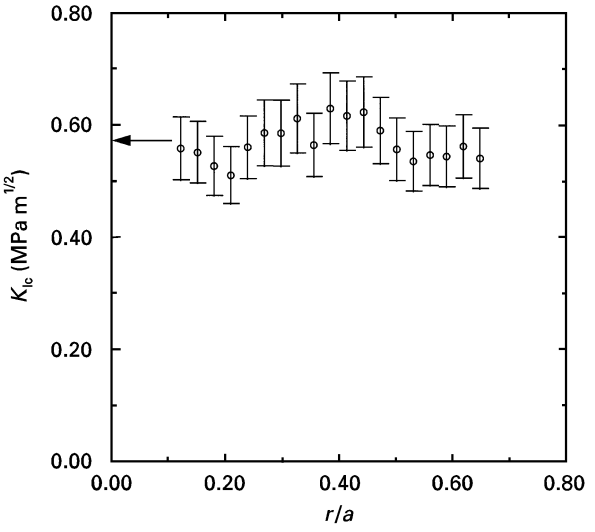

Figure 5 Fracture toughness values obtained from open-crack shape measurements in glass. The independence of the toughness values from position along the crack indicates a good match of the calculated crack shape with measurements.

3. Results

Figs 6 and 7 show micrographs of the porous RBSN with indentation-induced cracks, demonstrating the open-crack configurations. Fig. 7 shows an example of the frequently observed bridging phenomenon of a ligament across the crack faces.

These indentations in the RBSN were produced by Vickers hardness indentors with 400 g loads, in materials which ranged in porosity from 10–30%. In each case, cracks were consistently produced with well-formed shapes, i.e. four straight radial cracks emanating from corners of indentations.

The calculated fracture toughness values as a function of porosity are shown in Fig. 8. As has been found in other porous material systems, fracture toughness values depend on the average porosity in an apparent exponential fashion [12]. If the fracture toughness is

TABLE I Values of K_{IC} for model materials

Material	Measured fracture toughness (MPa m$^{1/2}$)	Previously reported fracture toughness (MPa m$^{1/2}$)
Soda-lime glass	0.81 ± 0.025	0.40–0.85
Silicon single crystal [1 1 0]	0.84 ± 0.03	0.87
α-Alumina single crystal [1 1 0]	2.86 ± 0.10	2.93[a]

[a] Value for h c p alumina.

a function of the porosity

$$K = K_0 \exp(-bp) \quad (2)$$

where p is the average porosity, then b is found to be 2.3, and compares well with data found in the literature

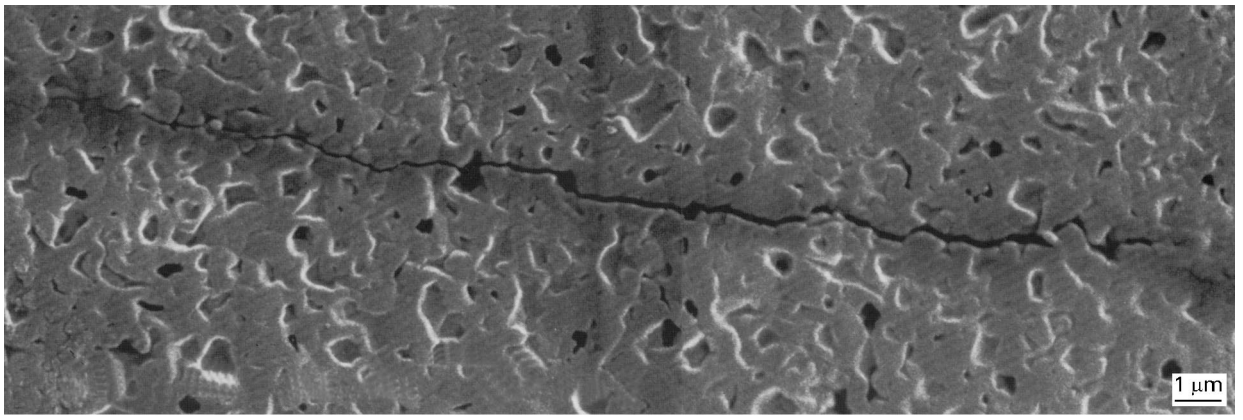

Figure 6 Micrograph of indentation-induced radial crack in RBSN.

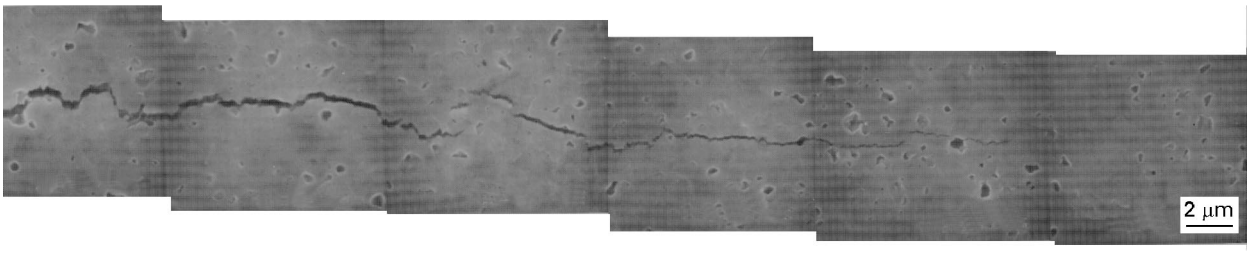

Figure 7 Micrograph of indentation-induced radial crack in high-porosity RBSN sample exhibiting high incidence of crack deflection and evidence of bridging ligaments.

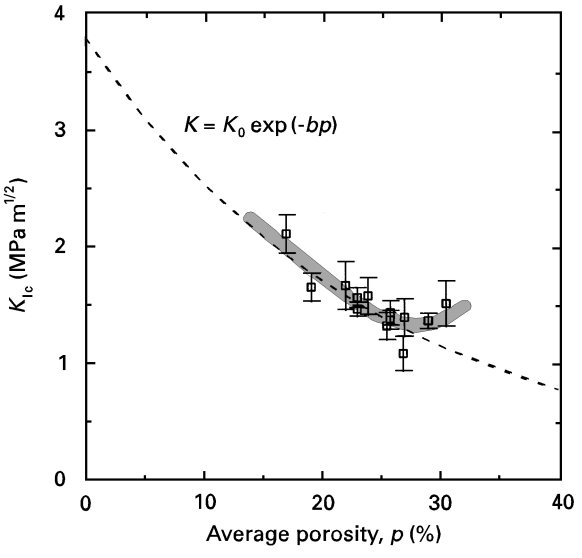

Figure 8 Dependence of fracture toughness on porosity in RBSN.

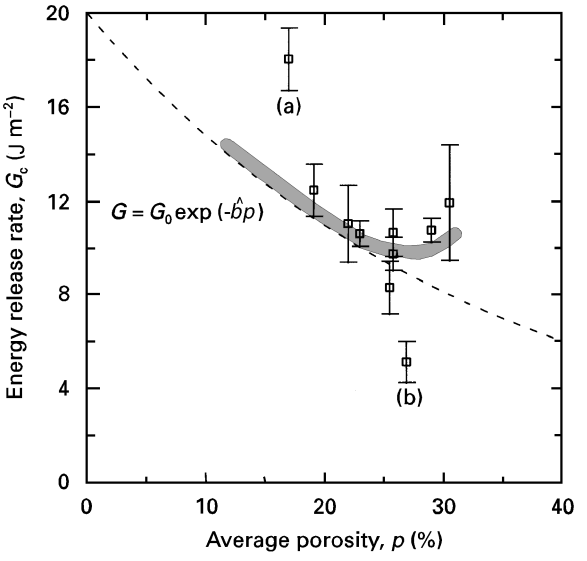

Figure 9 Dependence of energy release rate on porosity in RBSN.

where $b = 2.4$ for a range of silicon nitrides. Energy release rates show this trend more clearly in Fig. 9. However, at the high-porosity extreme, the toughness values tended to deviate considerably from the overall trend. This deviation correlates with the observation of a discernible increase in crack tortuosity in the highest porosity materials, as seen in Fig. 7.

The two exceptions to the overall trend are due to distinctly different processing steps. In material (a) a binder was added that increased the final density, and was postulated to create a final microstructure with more integrity. Material (b) exhibited large-scale channel-shaped pores which provided preferential fracture paths. Nominally, this material was produced with a slightly higher concentration of fine agglomerates which reduced the overall material homogeneity.

4. Discussion and conclusion

In the present experimental study we have utilized a theoretically well-known tool for determining the critical stress intensity for crack growth from the measurement of open-crack shapes. The method has been shown to possess good accuracy with some

chosen model materials with well-defined toughness values and has higher resolution than some previous methods involving measurement of indentation crack lengths associated with indentation load measurements. In the latter determinations of fracture toughness based on indentation loads, large uncertainties often exist resulting from frictional resistances which have no role in the propagation of the indentation-induced cracks. In comparison, the crack-shape measurement employed by us avoids such pit-falls by relying entirely on the direct measurement of relative displacement gradients along the crack, which are linked to the critical crack-tip stress intensity. The clear advantage of the method which has uncertainties less than 3%, are to some degree offset by the increased effort required in preparing high-resolution micrographs.

The method of measuring K_{IC} through measurement of crack shape was utilized here to determine influences of specific processing steps on the fracture toughness of a series of porous silicon nitrides based primarily on their relative porosities. While other methods of measuring the fracture toughness on small-size RBSN specimens indicated negligible differences, small, but definite, fracture toughness differences could be reliably resolved with the new technique. The measurements established a definite trend of decreasing toughness with increasing average porosity which has been commonly found in other studies as well [12]. However, at the highest levels of porosity, where high crack tortuosity was found, fracture toughness values deviated significantly upward from this decreasing trend. This effect appeared to be due to increased occurrence of crack deflection and of crack-face bridging ligaments in the high-porosity materials.

Acknowledgements

This research was supported by the AFOSR under Grant AFOSR-91-0263C, and for this support we thank Drs G. Haritos and W. Jones of that agency.

References

1. J. S. HAGGERTY, A. LIGHTFOOT, J.E. RITTER, P. A. GENNARI and S. V. GARVEY, *J. Amer. Ceram. Soc.* **72** (1989) 1675.
2. S. V. NAIR, P. CAI, J. E. RITTER, A. LIGHTFOOT and J. S. HAGGERTY, in "16th Annual Conference on Composites and Advanced Ceramics", Cocoa Beach, FL, January 1992 (American Ceramic Society, Westerville, OH) p. 90.
3. Z. LI, A. GHOSH, A. S. KOBAYASHI and R. C. BRADT, *J. Amer. Ceram. Soc.* **72** (1989) 904.
4. I. J. McCOLM, "Ceramic Hardness" (Plenum Press, New York, 1990) Ch. 5.
5. A. G. EVANS and E. A. CHARLES, *J. Amer. Ceram. Soc.* **59** (1976) 371.
6. G. R. ANSTIS, P. CHANTIKUL, B. R. LAWN and D. B. MARSHALL, *ibid.* **64** (1981) 539.
7. B. R. LAWN, A. G. EVANS and D. B. MARSHALL, *ibid.* **63** (1980) 574
8. R. F. COOK and G. M. PHARR, *ibid.* **73** (1990) 787.
9. S. S. CHIANG, D. B. MARSHALL and A. G. EVANS, *ibid.* **63** (1982) 298.
10. *Idem*, *ibid.* (1982) 312.
11. F. G. HAUBENSAK, A. LIGHTFOOT and J. S. HAGGERTY, *J. Mater. Sci.* submitted.
12. R. W. RICE, in "Treatise on Materials Science and Technology", Vol II, edited by R. K. MacCrone (Academic Press, New York, 1977) p. 199.

Received 16 February
and accepted 31 July 1996